Efficient numerical model for the computation of impedance functions of inclined pile groups in layered soils*

Guillermo M. Álamo[1], Alejandro E. Martínez-Castro[2], Luis A. Padrón[1], Juan J. Aznárez[1,*], Rafael Gallego[2], Orlando Maeso[1]

[1] Insituto Universitario de Sistemas Inteligentes y Aplicaciones Numéricas en Ingeniería (SIANI), Universidad de Las Palmas de Gran Canaria, Edificio Central del Parque Científico y Tecnológico, Campus Universitario de Tafira 35017 Las Palmas de Gran Canaria, Spain
guillermo.alamo / luis.padron / juanjose.aznarez / orlando.maeso @ulpgc.es

Departamento de Mecánica de Estructuras e Ingeniería Hidráulica, ETS de Ingenieros de Caminos, Canales y Puertos, Universidad de Granada, Avenida Fuentenueva s/n, 18002 Granada, Spain
amcastro / gallego @ugr.es

Abstract

This paper introduces a numerical model to obtain the time-harmonic dynamic response of pile foundations in non-homogeneous soils. The model is based on the integral formulation of the elastic problem and the use of Green's functions for the layered halfspace, and considers the soil as a group of zoned homogeneous, linear, isotropic, viscoelastic layers. The piles, on the other hand, are treated by finite elements as Timoshenko beams. Both formulations are coupled through the required compatibility and equilibrium equations along each pile. After being validated against previous results from the literature, the model is used to study the effects of soil non-homogeneity on the impedance functions of inclined piles and pile groups by considering different soil profiles whose properties vary with depth following a generalized power law. The impedance functions for three representative non-homogeneous soils are presented and compared with the ones of related homogeneous soils. Significant differences appear between the two situations for all studied rake angles. The magnitude of these differences strongly depends on the frequency range considered, specially for the case of pile groups, which shows the necessity of analysing the problem using soil profiles as close as possible to the actual depth-varying ones.

Keywords: Inclined piles, Impedance functions, Layered soil, Green's functions, Integral formulation

*Draft of the paper published in ENGINEERING STRUCTURES, 126, 379-390 (2016), DOI: 10.1016/j.engstruct.2016.07.047

1 Introduction

In situations where loads with great horizontal components are present inclined piles are used in combination with vertical piles to increase the foundation lateral stiffness. For the last decades, the use of inclined piles in seismic events have been strongly discouraged by several codes [1, 2] due to the bad performance observed in various earthquakes during the 90's. Nevertheless, in the last years the use of inclined piles has increased again and some studies have revealed that they might have a beneficial effect not only for the foundation, but for the superstructure too [3–6]. However, further study is needed in order to achieve a better understanding of the dynamic behaviour of raked pile foundations.

Despite the fact that seismic response of inclined piles has been the object of analysis for different studies [e.g. 5–10], the impedance problem of this type of pile foundation has received little attention. Impedance functions for specific configurations of inclined pile groups were studied by Mamoon et al. [11] for a 3×3 pile group with a rake angle of $\theta = 15^o$. Padrón et al. presented a complete set of impedance functions for configurations of single piles and pile groups embedded in an homogeneous halfspace [12] and in a soil layer resting on a bedrock [13]. A strong dependence on the configuration and rake angle was found for the group impedances, specially in the rocking and cross horizontal-rocking ones. Model tests on a single battered pile [14] and a 2×2 group [15] in dry cohesionless soil were carried out by Goit and Saitoh. In the first study, a comparison with a FEM numerical model was made, while in the latter the effects of soil non-linearity were analysed. In their recent work, Dezi et al. [16] introduced a numerical model for the analysis of pile foundations in layered soil deposits and presented impedance functions for 2×2 inclined pile groups embedded in an homogeneous soil deposit and in a two-layered soil deposit over a rigid bedrock.

In the aforementioned papers only homogeneous halfspaces or up to two-layered soil deposits were considered. However, real soils can present properties that vary with depth and the assumption of soil homogeneity can lead to misleading predictions of the foundation behaviour in the actual profile. Up to the authors' knowledge, only Giannakou et al. [17] have presented dynamic impedances for a single inclined pile in a soil profile whose properties vary continuously with depth.

For vertical pile foundations in non-homogeneous soils, the impedance problem has been studied by several authors with different methodologies. Velez et al. [18] employed a FEM formulation to obtain the lateral impedance of a single end-bearing pile in a non-homogeneous soil deposit overlaying a rigid bedrock. The results for the non-homogeneous media were compared against the ones corresponding to an 'statically equivalent' homogeneous deposit, showing that the static equivalence does not guarantee identical pile response under dynamic loads. Kaynia and Kausel [19], followed by Miura et al. [20], used a three-dimensional formulation based on Green's functions of cylindrical loads in layered semi-infinite media and presented a wide set of results for single piles and pile groups embedded in different soil profiles. Their results revealed that the horizontal impedance is more affected by near-surface soil properties than the vertical one, and that the interaction effects between the group piles are more pronounced in the non-homogeneous medium. Mylonakis and Gazetas [21, 22] presented a Winkler model to solve this problem. For pile groups, the pile-soil-pile effects were considered through interaction factors [23, 24] which relate the response of a 'receiver' pile to the oscillation of a near ('source')

pile. The behaviour of the non-homogeneous media was represented by a transfer-matrix formulation [25, 26]. The same methodology has been used by other authors to handle the impedance problem in non-homogeneous media [27–29]. In their recent work, Rovithis et al. [29] studied the lateral impedance of a single pile in a soil profile with properties varying according to a power law. Their results showed that lateral damping is overestimated when using the homogeneous assumption, leading to an un-conservative evaluation of the lateral pile deflections at high frequencies. This conclusion agrees with the results obtained by Giannakou et al. [17] for a lineal-varying non-homogeneous soil with a FEM model.

2 Efficient integral model for the dynamic analysis of inclined piles foundations

This paper describes an efficient model for the computation of impedance functions of inclined piles and pile groups in layered soils. The presented procedure is inspired by a previous formulation developed by Padrón et al. [30, 31], now using the Green's functions developed by Pak and Guzina [32] for the layered halfspace instead of the fundamental solution for the homogeneous entire space [33]. These Green's functions verify the free-surface, layer interfaces and radiation conditions. Thus, the proposed model avoids the need to discretize any boundary, which significantly reduces both the computational requirements and the numerical errors derived from the surface meshing. The model can be applied to study soils whose properties vary continuously with depth by modelling the continuous non-homogeneity through multiple zoned-homogeneous horizontal layers.

2.1 Model hypotheses

Inclined piles are modelled by finite elements as Timoshenko beams with hysteretic damping and neglecting their torsional resistance, while soil is considered as a semi-infinite region with different homogeneous, linear, isotropic, viscoelastic horizontal layers. The soil complex shear modulus μ_s is defined by the hysteretic damping coefficient β, as $\mu_s = Re[\mu_s](1 + 2\beta\mathrm{i})$, being i the imaginary unit. Welded boundary contact conditions at the pile-soil interfaces are assumed.

The proposed model assumes that soil continuity is not altered by the presence of piles, considering the tractions in the pile-soil interface as loads applied within the halfspace in the integral representation of the soil. This idea has already been used by previous static [34–36] and dynamic [30, 31] models.

2.2 Piles equations

The differential equation that determines the pile behaviour under dynamic loads has the following expression:

$$\mathbf{M}\ddot{\mathbf{u}}(t) \; + \; \mathbf{C}\dot{\mathbf{u}}(t) \; + \; \mathbf{K}\mathbf{u}(t) \; = \; \mathbf{f}(t) \tag{1}$$

where $\mathbf{M}$, $\mathbf{C}$ and $\mathbf{K}$ are the mass, damping and stiffness matrices respectively, $\mathbf{u}(t)$ the vector of nodal displacements and $\mathbf{f}(t)$ the vector of external nodal loads. Considering

harmonic loads ($\mathbf{u}(t) = \mathbf{u}\mathrm{e}^{\mathrm{i}\omega t}$ and $\mathbf{f}(t) = \mathbf{F}\mathrm{e}^{\mathrm{i}\omega t}$) and hysteretic damping defined by the pile damping coefficient ζ:

$$\mathbf{K}^* = \mathbf{K}(1 + 2\zeta\mathrm{i}) \tag{2}$$

eq. (1) can be expressed as:

$$\bar{\mathbf{K}}\mathbf{u} = \mathbf{F} \quad \text{with} \quad \bar{\mathbf{K}} = \mathbf{K}^* - \omega^2\mathbf{M} \tag{3}$$

where $\mathbf{u}$ and $\mathbf{F}$ are the vectors of nodal displacements and loads amplitudes and ω the excitation frequency.

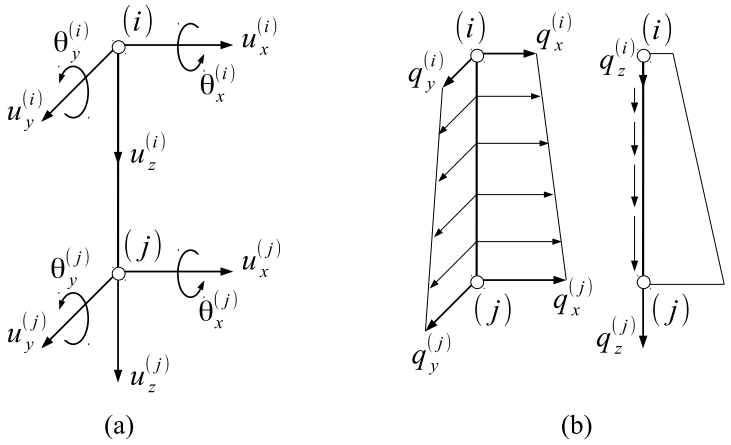

Figure 1: FEM pile elements. (a) Definition of degrees of freedom. (b) Linear approximation of tractions along the elements

Piles are discretized into 10 degrees-of-freedom 2-noded elements (Fig. 1(a)). Cubic shape functions for lateral displacements and quadratic shape functions for rotations, all satisfying the homogeneous static equation of the Timoshenko beam, are used [37]. For longitudinal displacements, linear shape functions are used. The stiffness and mass (translational plus rotational) matrix coefficients are obtained through the Hamilton's principle and are detailed together with the shape functions in [37]. As the piles are assumed not to affect the soil continuity, a reduced density must be considered for the piles (by subtracting the soil density: $\bar{\rho}_p = \rho_p - \rho_s$) in order not to overestimate the total system mass. A similar consideration was assumed in [24, 30].

The external forces acting over the pile can be separated into:

$$\mathbf{F} = \mathbf{F}^{top} + \mathbf{F}^{eq} \tag{4}$$

where $\mathbf{F}^{top}$ are the external forces at piles head and $\mathbf{F}^{eq}$ are the equivalent nodal forces due to the soil-pile interaction which are obtained as $\mathbf{F}^{eq} = \mathbf{Q}\ \mathbf{q}^p$, where $\mathbf{Q}$ is the matrix that transforms nodal values of distributed tractions along the pile ($\mathbf{q}^p$) into equivalent nodal forces.

The coefficients of the matrix $\mathbf{Q}$ are obtained by using the principle of virtual displacements and the traction and displacement shape functions. As the soil-pile interaction

distributed tractions $\mathbf{q}^p$ over the pile are modelled by linear shape functions (Fig. 1(b)), the lateral and axial components of the matrix are:

$$\mathbf{Q}^l = \frac{L_e}{1+\phi}\begin{bmatrix} (\frac{7}{20}+\frac{\phi}{3}) & (\frac{3}{20}+\frac{\phi}{6}) \\ L_e(\frac{1}{20}+\frac{\phi}{24}) & L_e(\frac{1}{30}+\frac{\phi}{24}) \\ (\frac{3}{20}+\frac{\phi}{6}) & (\frac{7}{20}+\frac{\phi}{3}) \\ -L_e(\frac{1}{30}+\frac{\phi}{24}) & -L_e(\frac{1}{20}+\frac{\phi}{24}) \end{bmatrix} \quad \mathbf{Q}^a = \frac{L_e}{6}\begin{bmatrix} 2 & 1 \\ 1 & 2 \end{bmatrix} \tag{5}$$

being L_e the pile element length and ϕ the ratio of the beam bending stiffness to the shear stiffness defined by:

$$\phi = \frac{24 I_p}{L_e^2 \alpha A_p}(1+\nu_p) \tag{6}$$

where I_p is the pile moment of inertia, A_p is the pile cross-section area, ν_p is the pile Poisson's coefficient and α is the shear coefficient that depends on the cross-section geometry, being $\alpha = 0.9$ for solid circular cross-sections. Note that for the yz plane the sign of the second and fourth rows of $\mathbf{Q}^l$ change due to the reference system used.

With all these considerations, the final FEM equation is of the form:

$$\bar{\mathbf{K}}\mathbf{u} - \mathbf{Q}\mathbf{q}^p = \mathbf{F}^{top} \tag{7}$$

where matrices $\bar{\mathbf{K}}$ and $\mathbf{Q}$ are global matrices obtained through the common assembly process of the corresponding elemental matrices. Pile inclination is handled through pre- and post- multiplying these elemental matrices by the appropriate rotation matrices.

2.3 Pak and Guzina's 3D Green's functions for a multilayered half-space

The benefits of the use of particular Green's functions in integral formulations of this problem was already observed, e.g., in the work of Matos Filho et al. [36], where the static halfspace Green's functions proposed by Mindlin [38] were used as fundamental solution, or previously, in the already mentioned work of Kaynia and Kausel [19] for piles driving in multilayered soils in dynamic regime.

In the model presented herein, the three-dimensional Green's function for the multilayered half space in time-harmonic dynamics has been implemented based on the solution developed by Pak and Guzina. The solution was published for the first time in [32], with important details in [39] and [40]. The main advantage of this solution comes from the fact that the propagator matrices include only bounded exponentials, avoiding numerical instabilities. The solution is built in three steps: i) displacement potentials; ii) angular Fourier transform; iii) radial Hankel transform. The computation of displacements and tractions requires a particular integration procedure to evaluate the inverse Hankel transform [32]. Also, a particular modification of the integration procedure, required at low frequencies, has been included based on the single layer solution derived by Martínez-Castro and Gallego [41].

These Green's functions were selected over other possibilities because of their numerical accuracy and fast convergence, due to the particular formulation of the propagation matrices involved, which are free of unbounded exponentials. However, other Green's functions for the layered halfspace can be found both for static [e.g. 42, 43] and dynamic [e.g. 44, 45] regimes.

2.4 Soil equations

The soil response is calculated through the dynamic reciprocal theorem [46], that allows to obtain an elastodynamic state by using another known solution. The known state used in this work is the Green's fundamental solution mentioned before. Attending to both the model and fundamental solution considerations, the dynamic reciprocal theorem integral expression simplifies to:

$$\mathbf{u}^{\kappa} = \int_{\Gamma_l} \mathbf{u}^{*} \mathbf{q}_l^s \, d\Gamma_l \tag{8}$$

where $\mathbf{u}^{\kappa}$ is the vector of displacements of the collocation point (κ), $\mathbf{u}^{*}$ the tensor that contains the fundamental solution when the unit load is placed at point κ and $\mathbf{q}_l^s$ are the tractions along the load line Γ_l.

The tractions $\mathbf{q}_l^s$ can be considered as the tractions at the soil-pile interface due to the soil-pile interaction experimented by the soil, while the displacements of the load line $\mathbf{u}$ correspond to the mid-line displacements of the piles.

Considering np pile lines and using linear shape functions to approximate the tractions along the soil-pile interface, eq. (8) can be rewritten into:

$$\mathbf{u}^{\kappa} = \sum_{m=1}^{np} \mathbf{G}_m \mathbf{q}_m^s \tag{9}$$

where the matrix $\mathbf{G}_m$ is obtained by integration of the fundamental solution times the shape functions over the pile m through a standard Gaussian quadrature and $\mathbf{q}_m^s$ is the vector containing the nodal values of the soil-pile tractions corresponding to the pile m.

The integral of the fundamental solution becomes singular when evaluated at the load line to which the collocation point belongs. To avoid this situation, a non-nodal collocation strategy using points on the fictional pile-soil interface is carried on as in Padrón et al. [12]. To satisfy the problem symmetry, four collocation points symmetrically placed around the pile axis are used as depicted in Fig. 2 (a). Considering the equations of displacements and rotations of the pile section to express the displacements of the collocation points in terms of those at the central nodes, and adding the resulting four sets of equations, eq. (9) for each pile node n becomes:

$$4\mathbf{u}^{(n)} = \sum_{k=1}^{4} \sum_{m=1}^{np} \mathbf{G}_m^k \mathbf{q}_m^s \tag{10}$$

where $\mathbf{G}_m^k$ is the matrix $\mathbf{G}_m$ when the unit load is placed at the interface point $k = 1, 2, 3, 4$.

This equation is applied to all pile nodes. However, for the first node (i.e. superficial node) of inclined piles, eq. (10) needs to be modified as the collocation strategy leads to collocation points placed out of the soil domain. As the fundamental solution is only defined for points within the soil, eq. (10) must be applied to an inner point c of the first pile element instead of to the first node, as illustrated in Fig. 2 (b). Then, the displacements of the inner point c are expressed in terms of the ones of the nodes of the first element through 3×10 matrix $\mathbf{\Psi}$, which contains the corresponding shape functions (evaluated at

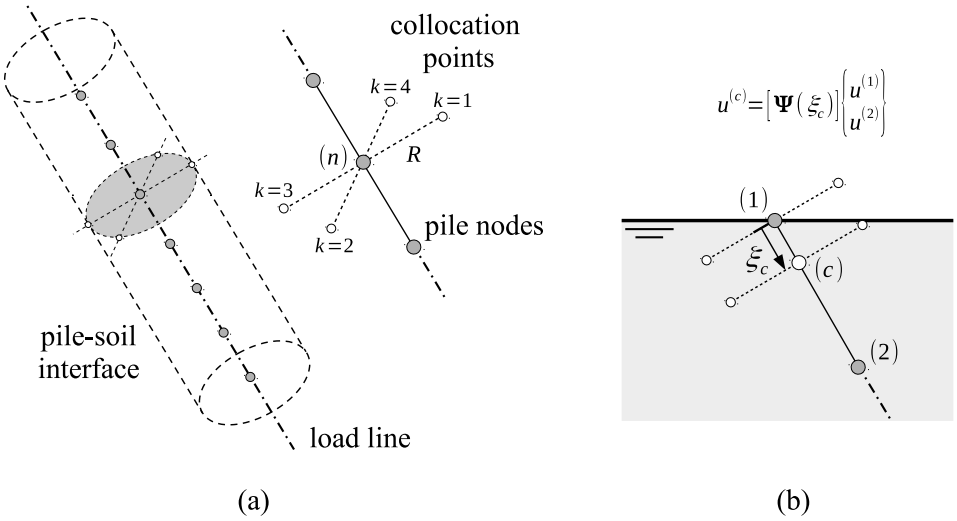

Figure 2: Non-nodal collocation strategy

the element local coordinate ξ_c) pre- and post- multiplied by the corresponding rotation matrices. Considering this, the discretized equation at such node becomes:

$$4\boldsymbol{\Psi}\left\{\begin{array}{c}\mathbf{u}^{(1)}\\ \mathbf{u}^{(2)}\end{array}\right\}=\sum_{k=1}^{4}\sum_{m=1}^{np}\mathbf{G}_m^k\mathbf{q}_m^s \tag{11}$$

Finally, the global soil equation can be expressed as:

$$4\boldsymbol{\Upsilon}\mathbf{u}=\mathbf{G}\mathbf{q}^s \tag{12}$$

where $\boldsymbol{\Upsilon}$ is a band matrix that contains either elements from $\boldsymbol{\Psi}_{3\times10}$ or $\mathbf{I}_{3\times3}$ depending on whether the corresponding equation is written for the first node of an inclined pile or not, and $\mathbf{G}$ is the global matrix obtained through the assembly of the elemental ones.

2.5 Soil-piles coupling

The presented formulations are coupled by imposing compatibility ($\mathbf{u}$) and equilibrium ($\mathbf{q}^s=-\mathbf{q}^p$) conditions along the pile lines. With these considerations, eq. (7) and (12) lead to the equation system:

$$\left[\begin{array}{cc}\bar{\mathbf{K}} & -\mathbf{Q}\\ 4\boldsymbol{\Upsilon} & \mathbf{G}\end{array}\right]\left\{\begin{array}{c}\mathbf{u}\\ \mathbf{q}^p\end{array}\right\}=\left\{\begin{array}{c}\mathbf{F}^{top}\\ 0\end{array}\right\} \tag{13}$$

that can be solved once boundary conditions (i.e. prescribed displacements or forces at pile top) are applied and the terms of the corresponding variables are rearranged.

3 Results

3.1 Soil definition

The soil profile is modelled as a viscoelastic unbounded region with constant density ρ_s, constant Poisson's ratio ν_s, constant hysteretic damping coefficient β_s and a varying shear wave velocity that increases continuously with depth along the pile length following the generalized power law function [47]:

$$c_s(z) = c_s^r \left(b + q\frac{z}{z^r}\right)^n \tag{14}$$

where b, q, n are dimensionless parameters that determine the soil non-homogeneity and z^r, c_s^r are the depth and shear wave velocity at the reference point. In the present study, the reference point is located at the pile tip ($z^r = L$) as assumed by several authors when treating non-homogeneity [e.g. 19, 20, 29]. However, some other researchers [e.g. 17, 18] consider the reference point at a depth equal to the pile diameter ($z^r = d$). These assumptions are equally valid but have to be carefully considered when comparing results.

Following Rovithis et al. [47], the general expression (14) can be rewritten in order to include the shear wave velocity at the surface (c_s^0) as:

$$c_s(z) = c_s^L \left[b + (1-b)\frac{z}{L}\right]^n \quad \text{with} \quad b = \left(\frac{c_s^0}{c_s^L}\right)^{1/n} \tag{15}$$

Using this expression, the soil profile depends upon two parameters: the ratio between the shear wave velocity at the surface and at the pile tip (c_s^0/c_s^L) and the non-homogeneity factor n. This factor is usually considered between 0 and 1, resulting in an homogeneous media when $n \to 0$ and in a linear variation of the shear velocity when $n \to 1$.

The shear wave velocity is kept constant for depths below the pile tip. As the soil density and Poisson's ratio are kept constant for the whole halfspace, the profile can be also expressed in terms of the soil Young's modulus as:

$$E_s(z) = \begin{cases} E_s^L \left[b + (1-b)\frac{z}{L}\right]^{2n} & \text{if} \quad 0 \le z \le L \\ E_s^L & \text{if} \quad z > L \end{cases} \tag{16}$$

where E_s^L corresponds to the soil Young's modulus at the reference point (i.e. the pile tip). Note that for a non-homogeneity factor $n = 0.5$, a linear variation with depth of the soil Young's modulus is obtained (Gibson soil).

3.2 Dynamic stiffness problem definition

The impedance functions (K_{ij}) are defined as the ratios between the steady-state force (or moment) applied at the pile cap and the resulting displacement (or rotation). In order to compute them, a unitary harmonic displacement (or rotation) is imposed to the group cap so the dynamic stiffness can be calculated by applying equilibrium with the forces at the pile heads. The impedance function is generally expressed through two frequency dependent coefficients representing the stiffness (k_{ij}) and damping (c_{ij}) components:

$$K_{ij} = k_{ij} + c_{ij} a_o i \tag{17}$$

where a_o is the dimensionless frequency corresponding to each particular case.

3.3 Verification results

3.3.1 Vertical piles in non-homogeneous media

In order to verify the ability of the presented formulation to address the impedance problem in non-homogeneous media, the results obtained for vertical elements by Miura et al. [20] of the horizontal, rocking and vertical impedances of a single vertical pile and 2×2 and 4×4 vertical pile groups in different soil types were reproduced.

The parameters that define the properties of the soil and piles are: Young's modulus ratio $E_p/E_s^L = 100$, density ratio $\rho_s/\rho_p = 0.7$, Poisson coefficient $\nu_s = 0.4$ for the soil and $\nu_p = 0.25$ for the piles and soil damping coefficient $\beta = 0.05$. The pile group geometry is defined by: piles aspect ratio $L/d = 20$ and distance ratio between adjacent pile centres $s/d = 5$. Three soil types are used (G1, G2 and G3 following the notation used by Miura et al.): two non-homogeneous soils with a linear variation of the Young's modulus value along the pile length ($n = 0.5$ with a value of $b = 0.1$ for G1 and $b = 0.4$ for G2) and a homogeneous soil (G3). All soil types keep the Young's modulus value constant and equal to E_s^L below the pile tip.

For simplicity's sake, only the comparison corresponding to the 2×2 group is shown in Fig. 3, where the stiffness and damping coefficients are presented against the dimensionless frequency $a_o = \omega\ d/c_s^L$. For the vertical and horizontal impedance problems, the coefficients are normalized by the pile static stiffness value k_{ij_0} times the number of piles. A different case is the one regarding the rocking impedances, where the contribution of the vertical static stiffness times the square of the distance to the rotation axis x_i is also included for this purpose. Note that this normalization is used only in this section in order to reproduce the results of [20]. A good agreement between the two methods can be seen for all soil types. The largest differences take place for the soil type G1 (the one with the highest properties variation), particularly for horizontal impedances.

The problems under study consider non-homogeneous soils whose properties vary continuously with depth (eq. 16); while the Green's functions used to solve the problem assume a finite number of zoned-homogeneous horizontal layers. Thus, the number of layers needed to model the continuously-varying soil must be assessed. Fig. 3 also presents the horizontal impedance functions obtained for different number of layers ($n_l = 4$, 10, 40 and 150), showing that, once a certain number of layer is reached, increasing the soil subdivision does not have any perceptible effect on the obtained results. The number of layers needed to achieve convergence depends on soil type, frequency range and problem type. In general, capturing adequately the impedance functions that involve horizontal components (i.e. horizontal, torsional and horizontal-rocking coupling ones) requires a larger number of layers: e.g. 30 layers were needed for the accurate computation of these impedances versus the 10 layers needed for the vertical and rocking problems. This convergence study has been done for all soil profiles employed in the current work. On the other hand, the developed model may present numerical instabilities when using very small elements to represent the piles. In order to avoid this issue, the ratio between the element diameter and length must be such that $d/L_e < 1.2$. All the results presented in this work are obtained using an element aspect ratio of $d/L_e = 1$, as a good compromise

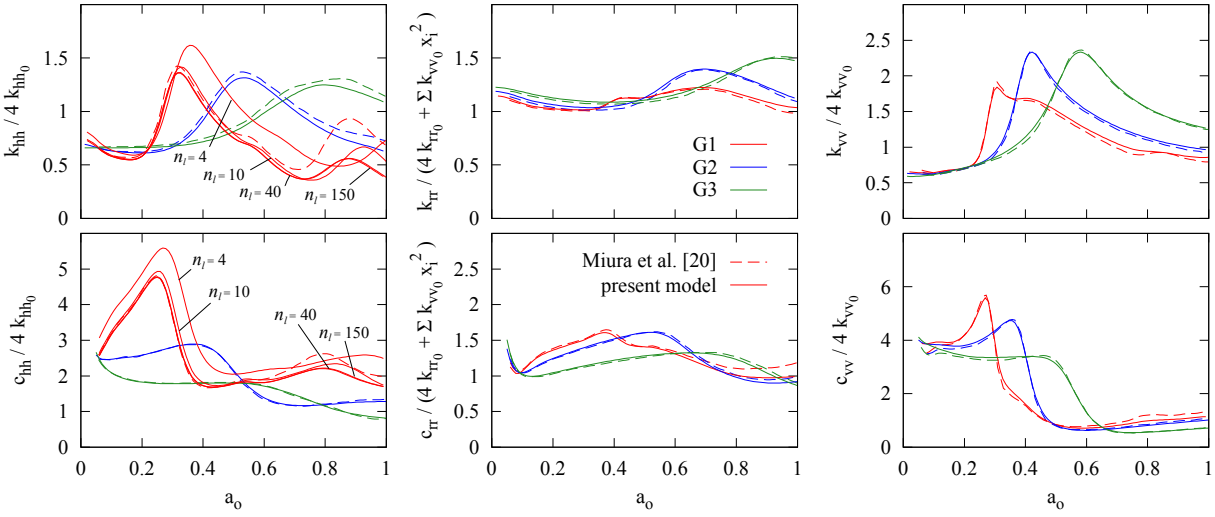

Figure 3: Horizontal, rocking and vertical impedances of a vertical 2 × 2 pile group. Comparison with the solution presented by Miura et al. [20]

between discretization and numerical stability.

3.3.2 Inclined piles in homogeneous media

On the other hand, in order to verify the implementation in case of the inclined piles, the impedance functions of a 2 × 2 pile group with inclined members presented by Medina et al. [48] are reproduced in Fig. 4, where the real and imaginary parts of the normalized impedances functions are plotted against the dimensionless frequency $a_o = \omega d/c_s$. The curves correspond to a foundation with $L/d = 15$ and $s/d = 7.5$ with the piles inclined θ degrees with respect to the vertical axis in the direction of the horizontal excitation. Pile-soil Young's modulus $E_p/E_s = 1000$ and density $\rho_s/\rho_p = 0.7$ ratios, soil $\nu_s = 0.4$ and pile $\nu_p = 0.25$ Poisson's ratios and soil hysteretic damping coefficient $\beta = 0.05$ are assumed. The results obtained by the proposed formulation agree very well with the ones obtained by Medina et al. using their BEM-FEM model.

3.4 Geometry and problem properties definition for the inclined pile foundations studied

The problem under study is sketched in Fig. 5. The foundations consist of one or more piles of equal length L, diameter d and material properties. In the group configurations, the space between two adjacent pile centres at cap level is defined by s. The rake angle θ measures the angle between the pile axis and the vertical.

The configurations studied correspond to the following properties: hysteretic damping coefficients $\beta_s = 0.05$ for soil and $\zeta = 0$ for piles; Poisson's ratios $\nu_s = 0.4$ for soil and $\nu_p = 0.25$ for piles; soil-pile density ratio $\rho_s/\rho_p = 0.7$ and pile aspect ratio $L/d = 15$. Two values of pile-soil modulus ratio $E_p/E_s^L = 10^3$ and 10^2 are studied in order to represent soft and stiff soils.

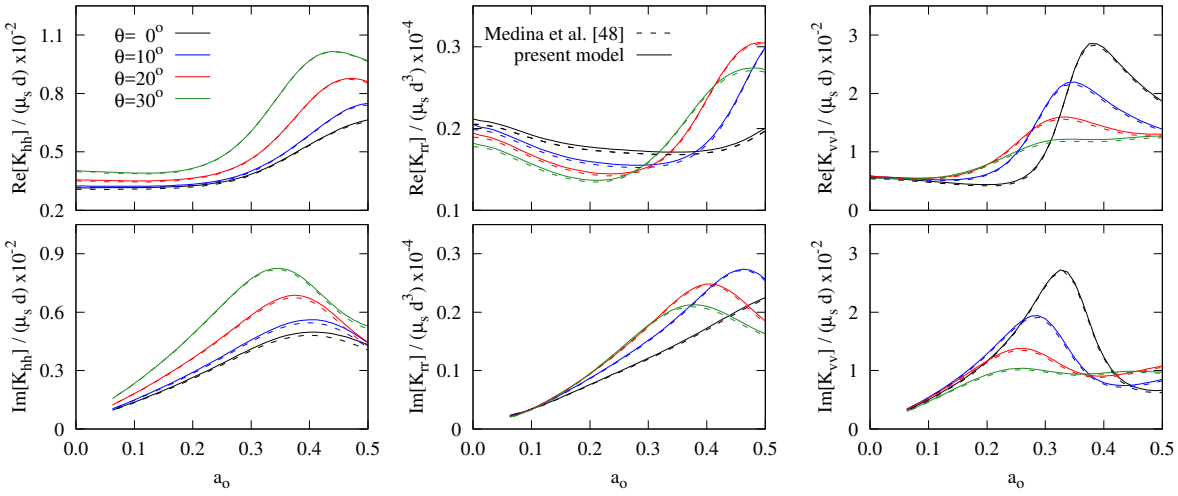

Figure 4: Horizontal, rocking and vertical impedances of 2×2 pile group with piles inclined in the direction of the horizontal excitation. Comparison with the solution presented by Medina et al. [48]

Results for the rake angles $\theta = 0^o$, 10^o, 20^o and 30^o are presented. The pile orientation can be parallel or perpendicular to the direction of excitation or along the cap diagonal (as indicated in each figure). For pile groups, separations between piles of $s/d = 5$ and 10 are considered.

3.5 Impedance functions for inclined piles in non-homogeneous media.

In order to study a wide set of non-homogeneous media, four values of the ratio between shear wave velocity at surface and pile tip ($c_s^0/c_s^L = 0.7$, 0.5, 0.25 and 0.1) are combined with three values of the non-homogeneity factor ($n = 0.3$, 0.5 and 0.9) resulting in 12 different soil profiles. In addition, impedances for the homogeneous soil are also computed so they can be used as reference values.

As the number of soil profiles is relatively large, and some of them yield similar results, four representative soils are chosen after having computed and compared all impedance functions. For this purpose, soil profiles that present similar impedance curves are grouped together, and the representative profile is selected as the closest to the group mean value. For this clustering process all of the configurations introduced in section 3.4 were considered. Fig. 6 shows the final soil clusters and their respective representative profiles (black solid lines).The variation of the shear wave velocity along the pile length is presented. The soil groups are arranged from left to right in ascending order of non-homogeneity.

In the following sections, normalized horizontal $K_{hh}/\bar{E}_s d$, rocking $K_{rr}/\bar{E}_s d^3$, vertical $K_{vv}/\bar{E}_s d$, torsional $K_{tt}/\bar{E}_s d^3$ and horizontal-rocking coupling $K_{hr}/\bar{E}_s d^2$ impedance functions are presented as functions of the dimensionless frequency $\bar{a}_o = \omega d/\bar{c}_s$. The mean shear wave velocity along the pile length $\bar{c}_s$ is used in order to handle the depth-varying

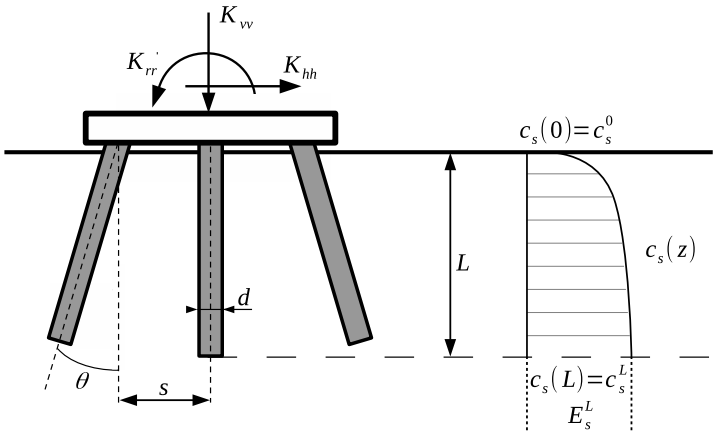

Figure 5: Problem definition

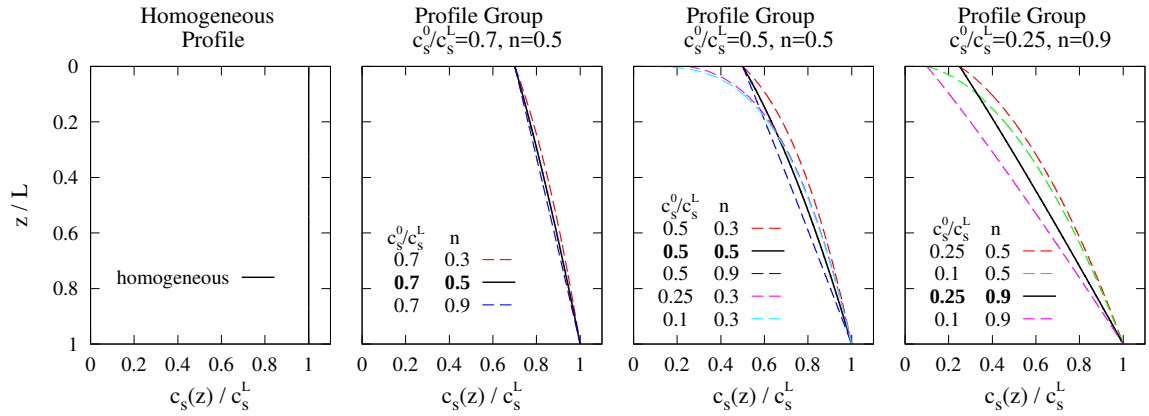

Figure 6: Soil profiles in terms of shear wave velocity. Each subplot presents all profiles yielding very similar impedance functions for the configurations proposed in section 3.4. The profile chosen as representative in each case is shown in black solid line

profiles:

$$\bar{c}_s = \frac{1}{L}\int_0^L c_s(z)\ \mathrm{d}z \tag{18}$$

In coherence with the normalization of the frequency, the mean value of the soil Young's modulus along the pile length $\bar{E}_s$ is used to obtain a dimensionless expression of the impedance functions. Due to space limitation, only a few of the obtained results are displayed. Thus, from the configurations of section 3.4, only impedance functions for single inclined piles and 3×3 inclined pile groups oriented both parallel and perpendicular to the horizontal component with a separation distance of $s/d = 5$ are presented for the representative soil profiles defined before. The 3×3 group is selected as its results clearly illustrate the effects of the soil non-homogeneity on the dynamic impedances of the pile groups. On the other hand, the case with inclination along the cap diagonal is omitted as its results can be extrapolated from the results corresponding to the two configurations

shown. Nevertheless, the impedance functions for all of the configurations described in section 3.4 can be found as additional material in the online version of this paper.

3.5.1 Inclined single pile impedance functions

Fig. 7 presents the impedance functions for a single pile inclined in the direction of the horizontal excitation. Note that for the rocking and horizontal-rocking cross impedances only the curves corresponding to vertical piles are presented as they are virtually insensitive to the rake angle.

The definition of the dimensionless frequency in terms of the mean shear wave velocity causes that the curves of the different soil profiles present similar evolutions with frequency, only scaling its value depending on the profile. For the horizontal impedance term, lower stiffness values are found as the soil non-homogeneity (as defined above) increases. The opposite effect is seen for the vertical, rocking and coupled terms, for which the normalized stiffness is higher for the non-homogeneous profiles.

The damping coefficients, on the other hand, present slightly smaller values as the soil non-homogeneity increases. This imply that, for non-homogeneous soils, the damping term is lower than the one corresponding to the homogeneous assumption, agreeing with the findings of previous works [17, 29]. This effect is manifested for all the angles of inclination. The only exception is found for the rocking and cross horizontal-rocking impedance functions, for which the damping component strongly increases depending on the soil non-homogeneity in the same sense as the stiffness term.

Regarding the effects of the rake angle: the horizontal impedance increases as the pile inclination augments due to the participation of the pile axial stiffness. This also explains why the vertical impedance decreases as the rake angle augments. This coupling between the horizontal and vertical components produces a horizontal-vertical cross impedance term arising for inclined piles. Contrary to what is found for the rest of impedance terms, the evolution with the frequency of the stiffness component of the vertical and horizontal-vertical cross impedances follows different trends depending on the soil stiffness: for soft soils ($E_p/E_s^L = 1000$), a reduction of the stiffness is seen as the frequency increases; while for stiff soils ($E_p/E_s^L = 100$), those stiffness terms augment continuously with this parameter.

3.5.2 Inclined 3×3 pile group impedance functions

Figs. 8 to 12 show the normalized impedance functions for the 3×3 pile groups with inclined elements for the studied soil profile sets. In general, the effects of the soil profile are the same for all of the group impedance functions: an average reduction in the stiffness and damping components and an increase in their dependence on the frequency as the soil non-homogeneity increases. These trends are the same for the curves corresponding to stiff (dashed lines) and soft soil configurations (solid lines).

The peaks on the impedances curves, produced due to resonance in the interaction between near piles, take place at smaller frequencies as the soil non-homogeneity increases. This effect make sense considering that if the wave velocity is reduced in the upper layers, the frequency at which resonance takes place should be reduced too. This effect is magnified with the increase in the rake angle as the distance between piles augments

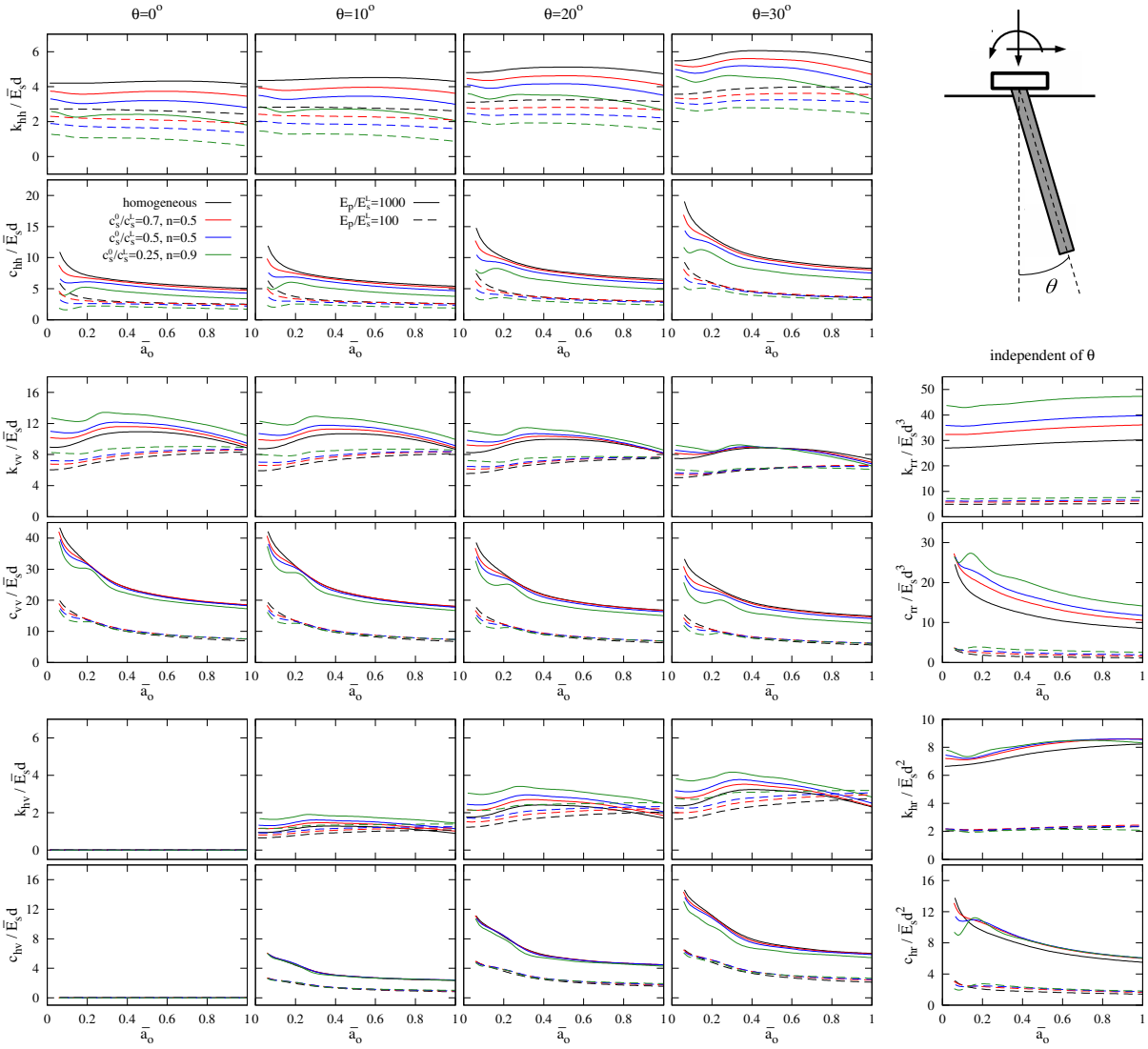

Figure 7: Impedance functions for a single inclined pile in different non-homogeneous media

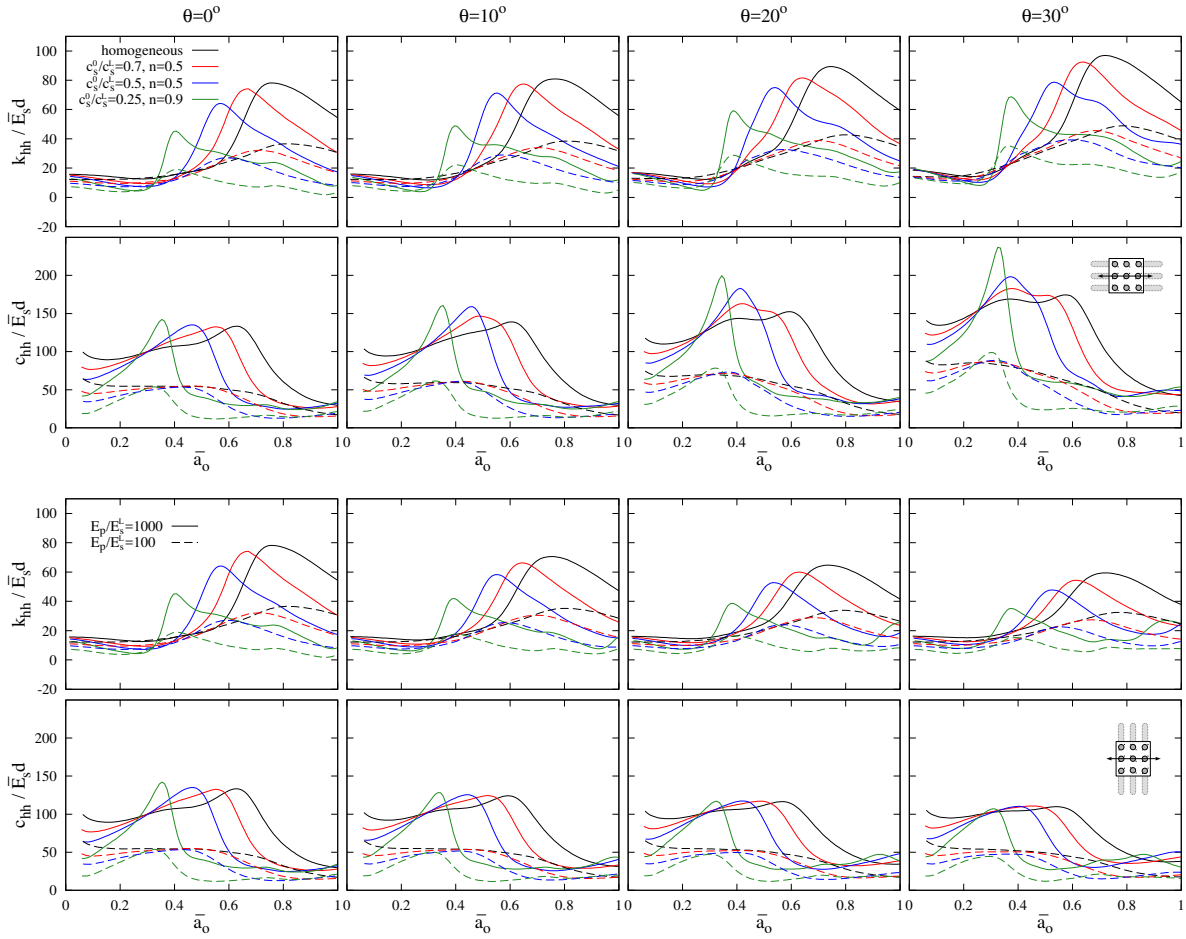

Figure 8: Horizontal impedance functions for a 3×3 group in different non-homogeneous media

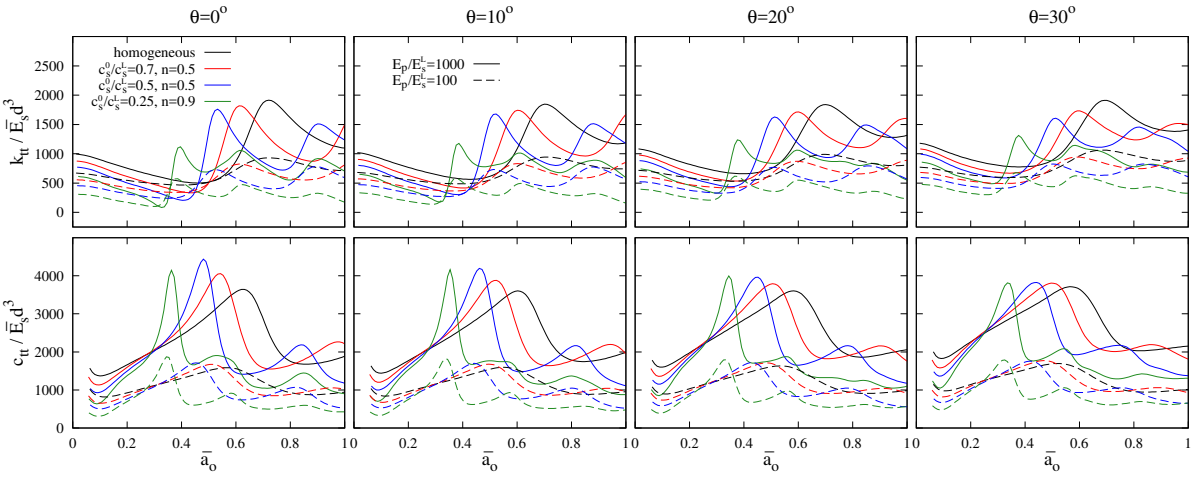

Figure 9: Torsional impedance functions for a 3×3 group in different non-homogeneous media

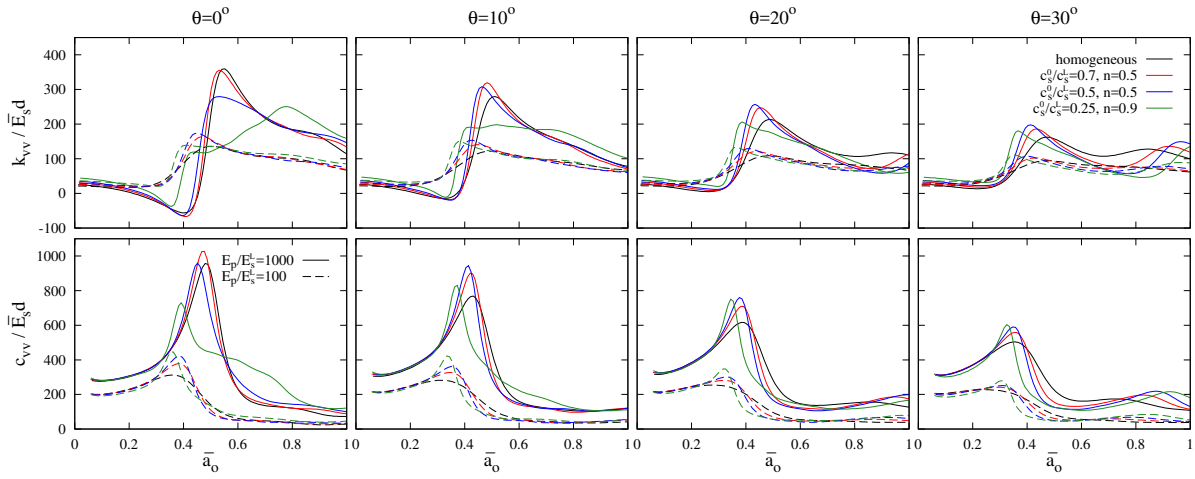

Figure 10: Vertical impedance functions for a 3×3 group in different non-homogeneous media

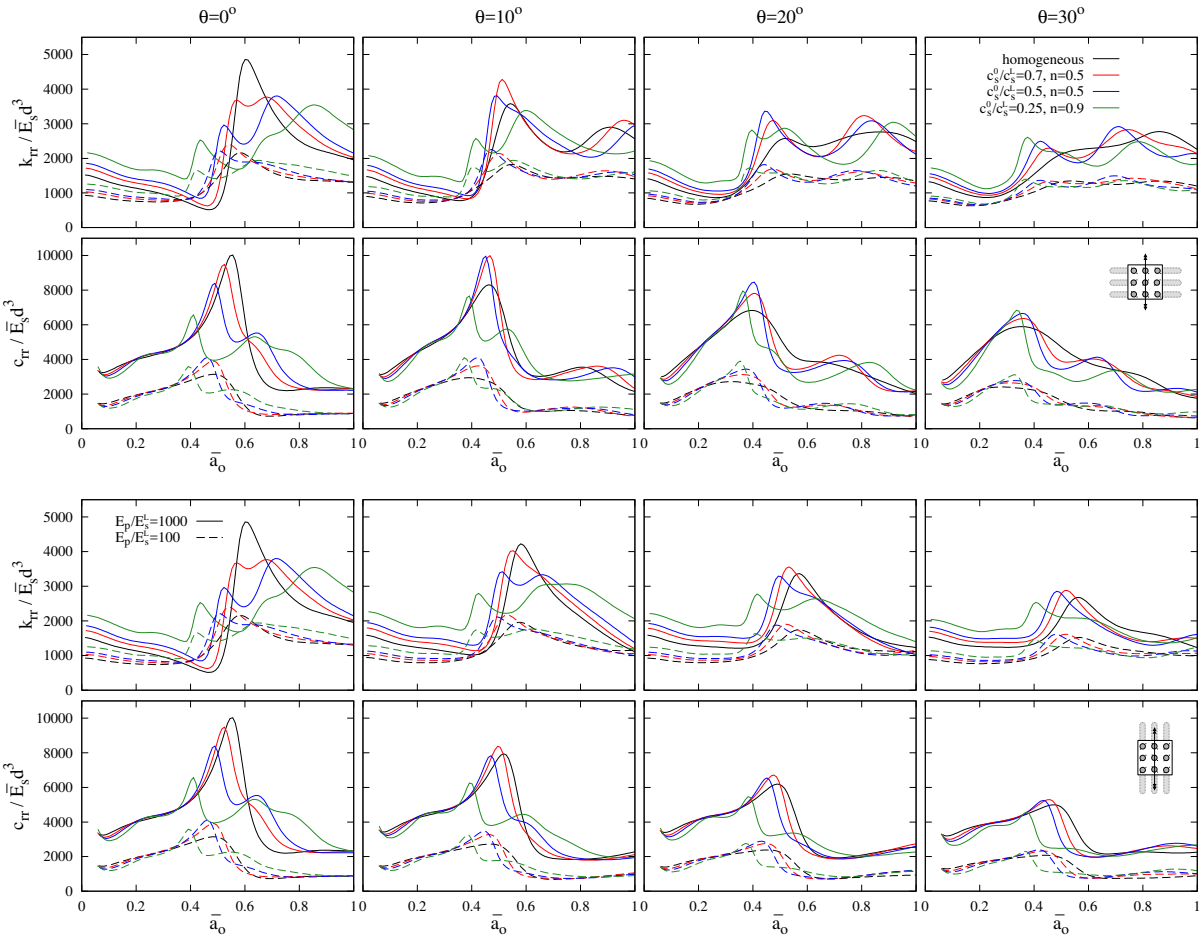

Figure 11: Rocking impedance functions for a 3×3 group in different non-homogeneous media

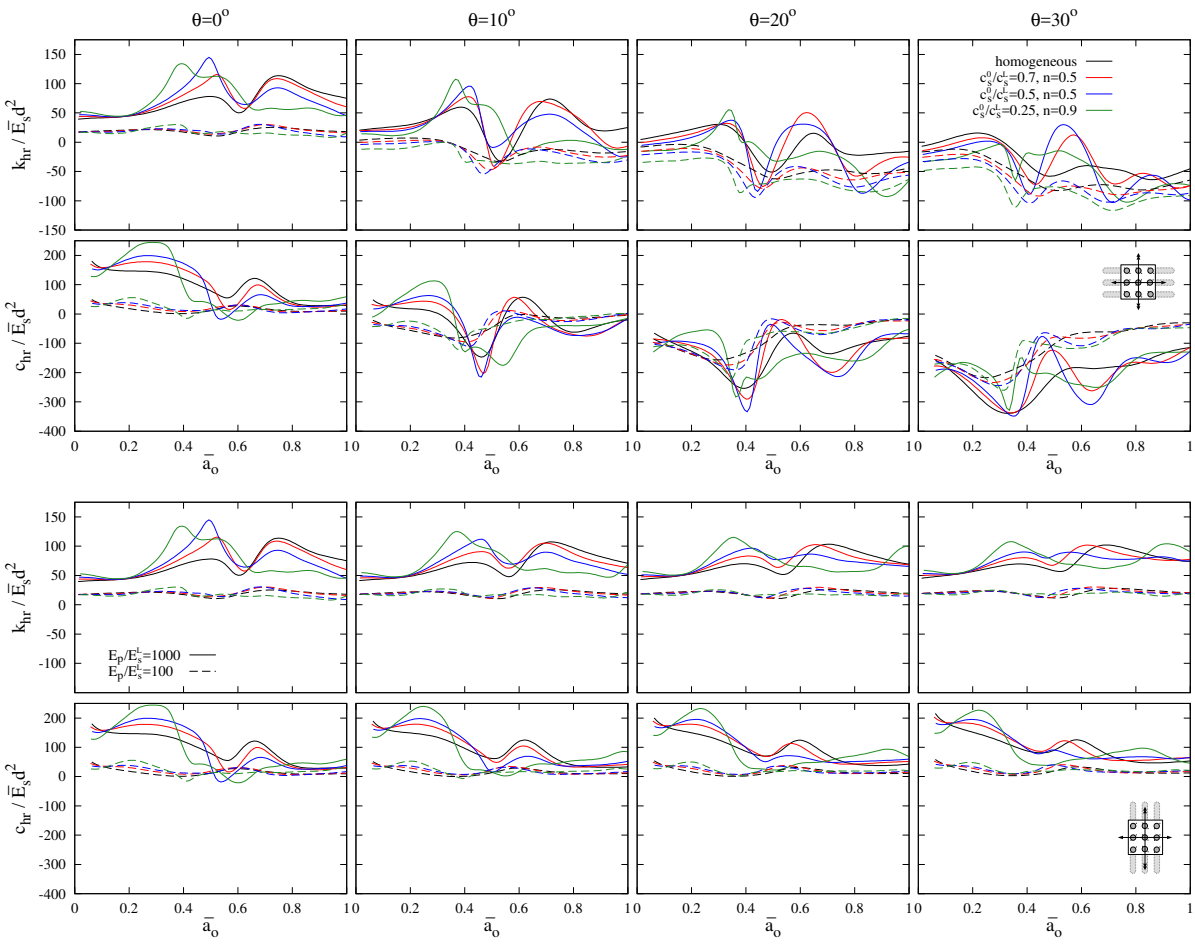

Figure 12: Horizontal-rocking coupling impedance functions for a 3×3 group in different non-homogeneous media

and, consequently, the frequency must be further reduced. Related to this effect, sharper peaks in the damping component at these frequencies can be seen as the non-homogeneity increases. This behaviour produces large differences at high frequencies between the damping component of the homogeneous media and the ones corresponding to the non-homogeneous profiles, even when a mean shear velocity is used for the definition of the dimensionless frequency.

However, the magnitude of the shift in the frequency at which those peaks appear is much larger for horizontal (Fig. 8) impedances than for the vertical (Fig. 10) modes, for which the peaks take place almost at the same dimensionless frequency regardless of the soil profile. Following Miura et al. [20], this can be explained assuming that the horizontal impedance is more affected by the superficial properties than the vertical one, which present a higher contribution of deeper soil properties.

Similar behaviour, in terms of frequencies at which the peaks are produced and the effects of the soil non-homogeneity, is seen between the vertical (Fig. 10) and rocking (Fig. 11) curves owing to the contribution of the former in the latter. This also happens between the horizontal (Fig. 8) and torsional (Fig. 9) impedance functions. In all of the mentioned curves, as the rake angle and the soil non-homogeneity increase, the interaction between distant piles becomes more important producing that new peaks arise.

Attending to the horizontal impedance curves (Fig. 8), different effects are seen depending on the direction of the pile inclination. When the piles are inclined perpendicular to the horizontal excitation, the stiffness and damping components decrease slightly with respect to the vertical pile configuration. On the other hand, if the piles are inclined parallel to the excitation, an increment in the impedance functions is found as the rake angle augments. Furthermore, the inclination of the piles parallel to the horizontal excitation intensifies the differences in the curve shapes between the studied profiles. Thus, the variability in the damping functions is highest for $\theta = 30^o$. Contrary to what happened for the single pile impedances, the soil profiles with depth-varying properties produce similar or even higher values of the maximum damping coefficient; while their stiffness component is significantly lower when compared to the homogeneous profile. Thus, for pile groups, the homogeneous assumption does not imply higher damping-stiffness ratios. This effect can also be seen for the torsional impedance functions, but not for the rest of terms. Noteworthy is the fact that these conclusions are obtained based on the normalization used: if the values of $\bar{E}_s$ and $\bar{c}_s$ used to normalize the frequency and the impedance components change, the stiffness component will vary in a greater extent than the damping one due to its definition (eq. 17).

Fig. 10 shows that, with the normalization employed, the vertical impedance functions for the homogeneous and $n = 0.5$ soil profiles are very close to each other, although their maxima do not appear at exactly the same dimensionless frequency. Both stiffness and damping functions for the most non-homogeneous profile ($n = 0.9$) converge to the results for the rest of profiles only for large rake angles ($\theta \geq 20^o$).

Owing to the great contribution of the vertical component to the rocking impedance functions, the effects of the normalization on the similarity of the curves described in the previous paragraph can also be seen in Fig. 11. However, these effects are manifested in a lower extent than for the vertical impedance curves. The rocking impedance curves strongly depend on the soil profile, presenting more peaks as the soil non-homogeneity

increases. This influence of the soil profile is stronger for piles with lower angles of inclination. Contrary to what was found for the horizontal impedance functions, an increase in the rake angle always produces a reduction in the rocking impedance value regardless of the direction of inclination. However, different curves are obtained depending on whether the piles are inclined parallel or perpendicular to the horizontal motion direction.

Regarding the cross horizontal-rocking component (Fig. 12), again different situations are seen depending on the direction of pile inclination. If the piles are inclined perpendicular to the excitation (bottom figures), the rake angle has virtually no influence on this impedance component. On the contrary, if the pile inclination is parallel to the excitation direction (top figures), the magnitude of the impedance values and its sign change as the angle increases, going from positive values for vertical piles to negative ones for higher inclination angles. This effect is produced for all the studied profiles.

4 Conclusions

This paper introduces a numerical model for the dynamic analysis of inclined piles foundations based on an integral formulation and the Green's functions for layered soils developed by Pak and Guzina [32]. The soil is modelled through the numerical integral approach while piles are represented by beam finite elements. As there is no need to discretize the soil surfaces, the presented model is efficient in terms of both computational requirements (specially memory usage) and mesh uncertainties, allowing its application to a wide variety of soil profiles. Besides, the proposed model can be further developed by including superstructures to the pile foundations or by considering other excitations such as seismic waves propagating through the soil (see details in [31]); being this the scope of authors future work.

The model has been validated against results that can be found in the literature for vertical piles in non-homogeneous soils [20] and for inclined piles in homogeneous media [48]. Once validated, the model has been used to obtain the impedance functions for inclined single piles and 2×2 and 3×3 pile groups with inclined elements embedded in different soils whose shear wave velocity varies along the pile length following a generalized power law. Attending to the computed results, three soils profiles are selected as representative of the twelve studied media and their corresponding impedance functions are compared with the ones of the homogeneous soil. These results are presented in a set of ready-to-use graphs that can be incorporated for the dynamic analysis of structures on pile foundations with inclined elements in non-homogeneous profiles. Up to the authors' knowledge, such a wide set of results covering these configurations has not yet been published in the literature.

From the analysis of the results presented: the impedance functions have been shown to strongly depend on the soil profile, which highlights the importance of estimating the ground real profile and the need of using it to accurately analyse the dynamic response of the foundation. Evidently, the magnitude of the stiffness functions tend to decrease when the mean shear wave velocity of the soil profile decreases, with the exception of the vertical mode, for which normalized impedance functions are largely independent of the soil profile, in the cases studied herein. The damping functions present, in general, the same behaviour. Also, and again with the exception of the vertical mode, the magnitude of the

stiffness function peaks and the frequencies at which they appear, decrease significantly when the non-homogeneity of the soil increases. It is noteworthy that the magnitude of the differences among the results corresponding to the different profiles diminishes for large pile rake angles. In any case, the equivalent homogeneous assumption can lead to impedance values that are significantly away from the ones that correspond to the actual soil profile depending on the frequency range of interest.

Acknowledgements

This work was supported by the Subdirección General de Proyectos de Investigación of the Ministerio de Economía y Competitividad (MINECO) of Spain and FEDER through research project BIA2014-57640-R. G.M. Álamo is a recipient of the FPU research fellowship FPU14/06115 from the Ministerio de Educación, Cultura y Deporte of Spain and a former recipient of the Program of predoctoral fellowship of the Universidad de Las Palmas de Gran Canaria. The authors would also like to thank the reviewers for their valuable comments which have helped to improve the manuscript.

References

[1] Eurocode 8: Design of structures for earthquake resistance. Part 5: Foundations, Retaining Structures and Geotechnical Aspects. European Committee for Standardization, Brussels. 2004.

[2] Récommendations AFPS 90. Association Française de Génie Parasismique. Presses del Ponts at chausées, Paris. 1990.

[3] Gazetas, G., Mylonakis, G.. Seismic soil-structure interaction: new evidence and emerging issues. In: Geotechnical Earthquake Engineering and Soil Dynamics III. Geotechnical Special Publication II. ASCE: New York; 1998, p. 1119–1174.

[4] Berrill, J.B., Christensen, S.A., Keenan, R.P., Okada, W., Pettinga, J.R.. Case study of lateral spreading forces on a piled foundation. Geotechnique 2001;51(6):501–517.

[5] Sadek, M., Isam, S.. Three-dimensional finite element analysis of the seismic behavior of inclined micropiles. Soil Dyn Earthq Eng 2004;24:473–485.

[6] Gerolymos, N., Giannakou, A., Anastasopoulos, I., Gazetas, G.. Evidence of beneficial role of inclined piles: observations and summary of numerical analyses. Bull Earthq Eng 2008;6(4):705–722.

[7] Giannakou, A., Gerolymos, N., Gazetas, G., Tazoh, T., Anastasopoulos, I.. Seismic behavior of batter piles: Elastic response. J Geotech Geoenviron Eng 2010;136(9):1187–1199.

[8] Isam, S., Hassan, A., Mhamed, S.. 3D elastoplastic analysis of the seismic performance of inclined micropiles. Comput Geotech 2012;39:1–7.

[9] Escoffier, S.. Experimental study of the effect of inclined pile on the seismic behavior of pile group. Soil Dyn Earthq Eng 2012;42:275–291.

[10] Medina, C., Padrón, L.A., Aznárez, J.J., Santana, A., Maeso, O.. Kinematic interaction factors of deep foundations with inclined piles. Earthq Eng Struct Dyn 2014;43(13):2035–2050.

[11] Mamoon, S.M., Kaynia, A.M., Banerjee, P.K.. Frequency domain dynamic analysis of piles and pile groups. J Eng Mech 1990;116(10):2237–2257.

[12] Padrón, L.A., Aznárez, J.J., Maeso, O., Santana, A.. Dynamic stiffness of deep foundations with inclined piles. Earthq Eng Struct Dyn 2010;39(12):1343–1367.

[13] Padrón, L.A., Aznárez, J.J., Maeso, O., Saitoh, M.. Impedance functions of end-bearing inclined piles. Soil Dyn Earthq Eng 2012;38:97–108.

[14] Goit, C.S., Saitoh, M.. Model tests and numerical analyses on horizontal impedance functions of inclined single piles embedded in cohesionless soil. Earthq Eng Eng Vib 2013;12(1):143–154.

[15] Goit, C.S., Saitoh, M.. Model tests on horizontal impedance functions of fixed-head inclined pile groups under soil nonlinearity. J Geotech Geoenviron Eng 2014;140(6).

[16] Dezi, F., Carbonari, S., Morici, M.. A numerical model for the dynamic analysis of inclined pile groups. Earthq Eng Struct Dyn 2016;45(1):45–68.

[17] Giannakou, A., Gerolymos, N., Gazetas, G.. On the dynamics of inclined piles. In: Proc. of the 10th International conference on Piling and Deep Foundations. Amsterdam, The Netherlands; 2006, p. 286–295.

[18] Velez, A., Gazetas, G., Krishnan, R.. Lateral dynamic response of constrained head piles. J Geotech Eng 1983;109(8):1063–1081.

[19] Kaynia, A.M., Kausel, E.. Dynamics of piles and pile groups in layered soil media. Soil Dyn Earthq Eng 1991;10(8):386–401.

[20] Miura, K., Kaynia, A.M., Masuda, K., Kitamura, E., Seto, Y.. Dynamic behaviour of pile foundations in homogeneous and non-homogeneous media. Earthq Eng Struct Dyn 1994;23(2):183–192.

[21] Mylonakis, G., Gazetas, G.. Vertical vibration and additional distress of grouped piles in layered soil. Soils Found 1998;38(1):1–14.

[22] Mylonakis, G., Gazetas, G.. Lateral vibration and internal forces of grouped piles in layered soil. J Geotech Geoenviron Eng 1999;125(1):16–25.

[23] Poulos, H.G.. Analysis of settlement of pile groups. Geotechnique 1968;18(4):449–471.

[24] Kaynia, A.M.. Dynamic stiffness and seismic response of pile groups. Research Report R83-03; Massachusetts Institute of Technology; Cambridge, MA; 1982.

[25] Thomson, W.T.. Transmission of elastic waves through a stratified solid medium. J Appl Phys 1950;21(2):89–93.

[26] Kausel, E., Rosset, J.M.. Stiffness matrices for layered soils. Bulle Seismol Soc Amer 1981;71(6):1743–1761.

[27] Lei, W.J., Wei, D.M.. Lateral impedances of single pile and pile groups in layered soils. Eng Mech 2004;21(5):36–40.

[28] Huang, M.S., Wu, Z.M., Ren, Q.. Lateral vibration of pile groups in layered soil. Chin J Geotech Eng 2007;29(1):32–38.

[29] Rovithis, E., Mylonakis, G., Pitilakis, K.. Dynamic stiffness and kinematic response of single piles in inhomogeneous soil. Bull Earthq Eng 2013;11(6):1949–1972.

[30] Padrón, L.A., Aznárez, J.J., Maeso, O.. BEM-FEM coupling model for the dynamic analysis of piles and pile groups. Eng Anal Bound Elem 2007;31(6):473–484.

[31] Padrón, L.A., Aznárez, J.J., Maeso, O.. 3-D boundary element-finite element method for the dynamic analysis of piled buildings. Eng Anal Bound Elem 2011;35(3):465–477.

[32] Pak, R.Y.S., Guzina, B.B.. Three-dimensional Green's functions for a multilayered half-space in displacement potentials. J Eng Mech 2002;128(4):449–461.

[33] Cruse, T.A., Rizzo, F.J.. A direct formulation and numerical solution of the general transient elastodynamic problem. I. J Math Anal Appl 1968;22(1):244–259.

[34] Mendonça, A.V., de Paiva, J.B.. A boundary element method for the static analysis of raft foundations on piles. Eng Anal Bound Elem 2000;24(3):237–247.

[35] Mendonça, A.V., de Paiva, J.B.. An elastostatic FEM/BEM analysis of vertically loaded raft and piled raft foundation. Eng Anal Bound Eleme 2003;27(9):919–933.

[36] Matos Filho, R., Mendonça, A.V., Paiva, J.B.. Static boundary element analysis of piles submitted to horizontal and vertical loads. Eng Anal Bound Elem 2005;29(3):195–203.

[37] Friedman, Z., Kosmatka, J.B.. An improved two-node timoshenko beam finite element. Comput Struct 1993;47(3):473–481.

[38] Mindlin, R.D.. Force at a point in the interior of a semi-infinite solid. J Appl Phys 1936;7(5):195–202.

[39] Guzina, B.B., Pak, R.Y.S.. On the analysis of wave motions in a multi-layered solid. Q J Mech Appl Math 2001;54(1):13–37.

[40] Guzina, B.B., Pak, R.Y.S.. Static fundamental solutions for a bi-material full-space. Int J Solids Struct 1999;36(4):493–516.

[41] Martínez-Castro, A.E., Gallego, R.. Three-dimensional Greens function for time-harmonic dynamics in a viscoelastic layer. Int J Solids Struct 2007;44(13):4541–4558.

[42] Kausel, E., Seale, S.H.. Static loads in layered halfspaces. J Appl Mech 1987;54(2):403–408.

[43] Pan, E.. Static Green's functions in multilayered half spaces. Appl Math Model 1997;21(8):509–521.

[44] Kausel, E.. Fundamental solutions in elastodynamics. A Compendium. Cambridge University Press; 2006.

[45] Luco, J.E., Apsel, R.J.. On the Green's functions for a layered half-space. Part I. Bull Seismol Soc Amer 1983;73(4):931–951.

[46] Wheeler, L.T., Sternberg, E.. Some theorems in classical elastodynamics. Arch Ration Mech Anal 1968;31(1):51–90.

[47] Rovithis, E.N., Parashakis, H., Mylonakis, G.E.. 1D harmonic response of layered inhomogeneous soil: Analytical investigation. Soil Dyn Earthq Eng 2011;31(7):879–890.

[48] Medina, C., Padrón, L.A., Aznárez, J.J., Maeso, O.. Influence of pile inclination angle on the dynamic properties and seismic response of piled structures. Soil Dyn Earthq Eng 2015;69:196–206.